Nonlinear Mixed-Effects Modeling of MNREAD Data

Sing-Hang Cheung,[1,2] *Christopher S. Kallie,*[2] *Gordon E. Legge,*[2] *and Allen M. Y. Cheong*[2]

Purpose. It is often difficult to estimate parameters from individual clinical data because of noisy or incomplete measurements. Nonlinear mixed-effects (NLME) modeling provides a statistical framework for analyzing population parameters and the associated variations, even when individual data sets are incomplete. The authors demonstrate the application of NLME by analyzing data from the MNREAD, a continuous-text reading-acuity chart.

Methods. The authors analyzed MNREAD data (measurements of reading speed vs. print size) for two groups: 42 adult observers with normal vision and 14 patients with age-related macular degeneration (AMD). Truncated sets of MNREAD data were generated from the individual observers with normal vision. The MNREAD data were fitted with a two-limb function and an exponential-decay function using an individual curve-fitting approach and an NLME modeling approach.

Results. The exponential-decay function provided slightly better fits than the two-limb function. When the parameter estimates from the truncated data sets were used to predict the missing data, NLME modeling gave better predictions than individual fitting. NLME modeling gave reasonable parameter estimates for AMD patients even when individual fitting returned unrealistic estimates.

Conclusions. These analyses showed that (1) an exponential-decay function fits MNREAD data very well, (2) NLME modeling provides a statistical framework for analyzing MNREAD data, and (3) NLME analysis provides a way of estimating MNREAD parameters even for incomplete data sets. The present results demonstrate the potential value of NLME modeling for clinical vision data. (*Invest Ophthalmol Vis Sci.* 2008; 49:828–835) DOI:10.1167/iovs.07-0555

Parametric characterization of a response function for individual patients can be important in assessment and diagnosis. However, such characterization is often difficult because of noisy or incomplete data as a result of the patient's limiting condition (e.g., test range restriction attributed to acuity or field reduction) or insufficient testing time. Mixed-effects modeling is a method of analyzing data from groups of people. In recent years, mixed-effects modeling has gained popularity in pharmaceutical, clinical, and behavioral studies.[1–4] Here we present nonlinear mixed-effects (NLME) modeling[5–7] of MNREAD data sets as a robust method of analyzing and summarizing reading speed data, even when the data are incomplete. Thereby, we demonstrate the potential value of NLME modeling for clinical vision data.

Improved reading ability is often the primary goal of vision rehabilitation for patients with low vision.[8] Precise measurements of reading performance provide valuable information for assessment[9–12] and rehabilitation evaluation.[13–15] Reading speed is measured as a function of print size in the MNREAD test.[16–20] Research has shown that reading speed increases sharply with print size at small print, plateaus at mid-range print, and decreases gradually at large print (>1.4 logMAR or 2° of visual angle; see Mansfield and Legge[21] for details on print size definitions and conversions).[22–24]

MNREAD is a continuous-text reading-acuity chart.[17,18,20] It has 19 sentences at print sizes from −0.5 to 1.3 logMAR in 0.1-log steps at a standard viewing distance of 40 cm, capturing the sharp rising part of the reading speed versus print size curve at small print and the asymptote at the mid-range print (Fig. 1). When the MNREAD chart is used at a closer viewing distance, the measured reading speed curve may also exhibit a decline at large print size.

The MNREAD curve is often approximated by a two-limb function composed of two straight lines.[22] Three key parameters are used to summarize the function[17,20]: maximum reading speed (MRS), critical print size (CPS, the smallest print size at which MRS can be attained), and reading acuity (RA, the smallest print size that can be resolved). These parameters have revealed important differences in reading performance among patients with age-related macular degeneration (AMD),[19] retinitis pigmentosa,[25] and dyslexia[26] compared with people with normal vision. Effects of children's grade level and age on these MNREAD parameters have also been found[12] (Cheung S-H, et al. *IOVS* 2006;47:ARVO E-Abstract 5830). Robust methods for estimating and analyzing the MNREAD curve provide the tools for answering important research questions about reading performance.

When the two-limb function is used to fit a set of MNREAD data, the CPS is defined as the intersection of the two lines. Thus, the estimation of the CPS hinges on the estimation of the slope of the rising line at small print. Mansfield et al.[19] pointed out that because of the rapid deterioration in reading speed at small print and noisier reading speed measurements near the acuity limit, the estimation of the rising slope can be poor and, thus, the accuracy and precision of the CPS estimates can be compromised. Moreover, as shown in Figure 1A, the elbow of the two-limb function fit is usually to the left of the observed data, tending to underestimate the CPS. In this study, we introduce an exponential-decay function to provide smooth fits for the reading speed versus print size data (Fig. 1B). Similar smooth nonlinear functions have also been used by other researchers[27] (Massof RW. *IOVS* 2003;44:ARVO E-Abstract 1284).

Although the MNREAD parameters have been shown to have high test-retest reliability,[28] parameter estimation may be difficult, or even impossible, when one person's data set is noisy or incomplete. For instance, acuity reduction or inadequate testing time may result in reading speed measurements for a compressed range of print sizes. Appropriate grouping of MNREAD data, for example by diagnosis, and NLME modeling of the MNREAD curves from appropriately defined groups of

From the [1]Department of Psychology, The University of Hong Kong, Hong Kong SAR, China; and the [2]Department of Psychology, University of Minnesota, Minneapolis, Minnesota.

Presented at the annual meeting of the Association for Research in Vision and Ophthalmology, Fort Lauderdale, Florida, May 2005.

Supported by National Institutes of Health Grant EY002934 (GEL).

Submitted for publication May 9, 2007; revised July 17 and October 22, 2007; accepted December 18, 2007.

Disclosure: **S.-H. Cheung**, None; **C.S. Kallie**, None; **G.E. Legge**, P; **A.M.Y. Cheong**, None

The publication costs of this article were defrayed in part by page charge payment. This article must therefore be marked "*advertisement*" in accordance with 18 U.S.C. §1734 solely to indicate this fact.

Corresponding author: Sing-Hang Cheung, Department of Psychology, University of Hong Kong, Pokfulam Road, Hong Kong SAR, China; singhang@hku.hk.

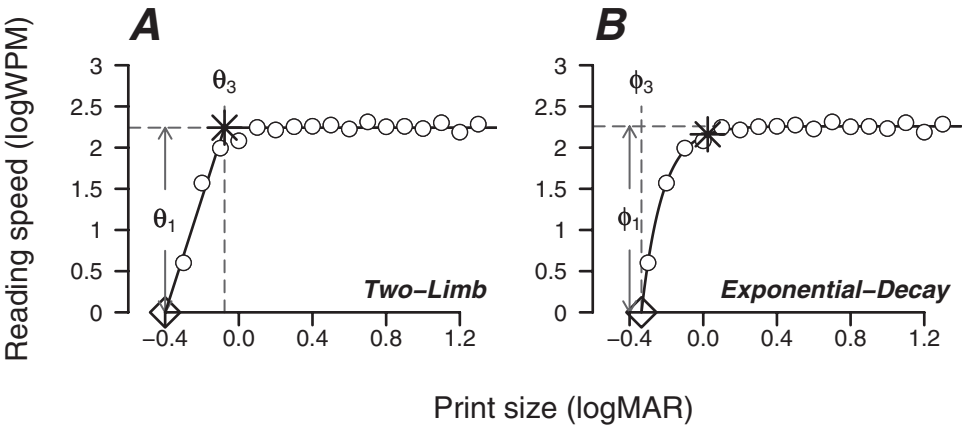

FIGURE 1. Illustration of the two functions. (**A**) *Two-limb* function. θ_1 denotes the MRS in logWPM, and θ_3 denotes the CPS. (**B**) *Exponential-decay* function. ϕ_1 denotes the MRS in logWPM, and ϕ_3 denotes the print size at which reading speed is 0 logWPM (i.e., 1 WPM). CPS is plotted as an *asterisk*, and reading acuity (RA) is plotted as a *diamond*.

patients can be a method for estimating parameters if data sets are incomplete. In clinical settings, when incomplete MNREAD data are collected, the new data set can be grouped with existing data sets from patients of similar conditions, and NLME modeling can be applied. We will illustrate NLME modeling of an incomplete data set produced by truncating complete sets of normal data and a data set from a group of patients with AMD.

To summarize the objectives of this study, we will (1) introduce an exponential-decay function that models MNREAD data, (2) introduce NLME modeling as a method of analyzing MNREAD data, and (3) show the advantage of using NLME when MNREAD data sets are incomplete.

METHODS

Participants

MNREAD data were collected from two groups of participants. The first group consisted of 42 adult observers with normal vision (25 women, 17 men), recruited for another study in the laboratory (Cheung S-H, et al. *IOVS* 2005;46:ARVO E-Abstract 4784). Their ages ranged from 19 to 65 years (mean, 33 ± 14 years). Best-corrected binocular visual acuity measured with the Lighthouse distance acuity chart (Optelec, US Inc., Vista, CA) was better than 20/20 for all observers in this group. They were all fluent English speakers. The second group consisted of 14 patients with a primary ocular diagnosis of AMD; their ages ranged from 65 to 87 years (mean, 78.6 ± 5.6 years). They were recruited from the Low Vision Center of the University of Minnesota and Vision Loss Resources (Minneapolis, MN), for another study in the laboratory.[29] All observers in this second group were native English speakers. Our AMD participants were considerably older than our normal-vision participants, but this study did not include any direct comparison between the two groups. Informed consent was obtained from each observer before testing. The protocol of this study followed the tenets of the Declaration of Helsinki and was approved by the Institutional Review Board of the University of Minnesota.

MNREAD Measurements

MNREAD Acuity Charts (Optelec, US Inc.) were used to measure reading speed as a function of print size. MNREAD measurements in both contrast polarities (i.e., black on white and white on black) were made on the normal-vision group but only in regular polarity (black on white) on the AMD group. The observers were asked to read aloud one sentence at a time, as the sentences were uncovered one by one from large to small print. The observers were asked to read as fast and as accurately as possible. Reading time and number of errors made for each sentence were recorded on a score sheet and were converted to reading speed in words per minute by the method described in the test instructions. Viewing distance was fixed at 40 cm for the normal-vision group or at a shorter distance, determined on an observer-by-observer basis, for the AMD group. A simulated incomplete data set was generated by randomly truncating data either on the rising slope (<CPS − 0.1 logMAR) or at the asymptote (>CPS + 0.1 logMAR) of the MNREAD curves in the normal-vision group.

Two-Limb Function versus Exponential-Decay Function

Two functions were used to model reading speed versus print size data in a log-log scale. The first function was a *two-limb* function, composed of two straight lines:

$$f(x) = \begin{cases} e^{\theta_2}(x - \theta_3) + \theta_1 & \text{if } x < \theta_3 \\ \theta_1 & \text{if } x \geq \theta_3 \end{cases}$$

where x represents the print size in logMAR, $f(x)$ the corresponding reading speed in log words per minute (logWPM), θ_1 the maximum reading speed (MRS) in logWPM, $\exp(\theta_2)$ the slope of the first limb (the slope of the second limb is 0), and θ_3 the CPS_{TL}. θ_3 is the intersection of the two straight lines. The slope of the first limb was parametrized as $\exp(\theta_2)$ to ensure positivity. The three parameters (θ_1, θ_2, and θ_3) were estimated using optimization procedures either through individual curve fitting or nonlinear mixed-effects (NLME) modeling.[5–7]

The second function was an *exponential-decay* function

$$g(x) = \phi_1(1 - e^{k})$$

$$k = -e^{\phi_2}(x - \phi_3)$$

where x represents the print size in logMAR, $g(x)$ the corresponding reading speed in logWPM, ϕ_1 the MRS in logWPM, $\exp(\phi_2)$ the rate of change in reading speed as a function of print size, ϕ_3 the print size at which reading speed is 0 logWPM (i.e., 1 WPM). The rate of change in the function was parametrized as $\exp(\phi_2)$ to ensure positivity. The three parameters (ϕ_1, ϕ_2, and ϕ_3) were estimated using optimization procedures through either individual curve fitting or NLME modeling.[5–7] The CPS_{ED} was defined as the print size that yielded a criterion percentage of the MRS. Linear regressions were calculated for the CPS_{ED} in the exponential-decay function at five different criterion reading speeds (75%–95% of the MRS) against the CPS_{TL} in the two-limb function.

Nonlinear Mixed-Effects Models of Reading Speed Data

Analyses of MNREAD data in a group of observers often involve two steps: curve fitting for each observer followed by statistical analyses (univariate or multivariate) on the estimated parameters. Mixed-effects

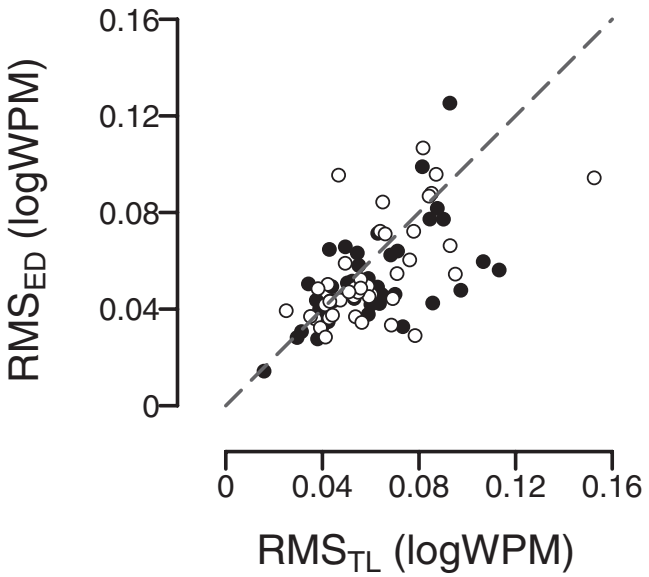

FIGURE 2. Plot of RMS errors for exponential-decay fits (RMS_{ED}) against RMS errors for two-limb fits (RMS_{TL}) for the normal-vision group. Data from the regular contrast polarity (black on white) data set are plotted as *filled circles*. Data from the reversed contrast polarity (white on black) data set are plotted as *open circles*. The *gray dashed line* is the equality line.

modeling is a powerful statistical framework for combining the two steps. Because the relationship between reading speed and print size is nonlinear, we analyzed MNREAD data using NLME models.[5–7] Fitting of NLME models involves an iterative process, in which the means of the different groups (fixed effects) and the variances within the groups (random effects) are estimated. Parameters for each individual data set are then estimated given the estimated means and variances. Details of the NLME models used in this study are included in the Appendix.

Statistical Analyses

Goodness-of-fit for the individual MNREAD curves was examined by analyzing the residuals (observed values − predicted values) and the root-mean-square (RMS) error (square root of the average squared residuals). We used bootstrap[30,31] in most of our statistical analyses with 10,000 resampling. All reported intervals (in parentheses) were 95% bootstrap confidence intervals ($CI_{bootstrap}$) estimated using the bias-corrected and accelerated percentile method (BC_a).[32]

RESULTS

Two-Limb Function versus Exponential-Decay Function

Figure 2 is a scatter plot of the RMS error from individual curve fitting (see Appendix for details) of the two-limb function (*x*-axis) and the exponential-decay function (*y*-axis) from the data set of the 42 observers with normal vision. RMS error from the two functions clustered around the equality line, with more data points below and to the right of the equality line, indicating that the exponential-decay function provided better fits (smaller errors). The average differences (95% $CI_{bootstrap}$ in parentheses) between the RMS errors from the two functions were 0.0079 (0.0026, 0.0138) logWPM and 0.0061 (0.0007, 0.0121) logWPM for regular contrast polarity (i.e., black on white) and reversed contrast polarity respectively. Although the differences were small, they were statistically significant ($ps_{bootstrap} \leq 0.05$).

The two left panels (A and C) of Figure 3 show the residuals as a function of print size for the two-limb (TL) fits and the exponential-decay (ED) fits in the normal-vision data set. Print sizes were adjusted relative to the critical print size. Because we wanted to compare the results on the residuals between the two function fits, the ED residuals were also adjusted to the CPS_{TL} instead of the CPS_{ED}. As shown in Figure 3A, residuals from TL fits tended to be negative around the CPS_{TL}, indicating that the data tended to lie below the fitted curve. The two right

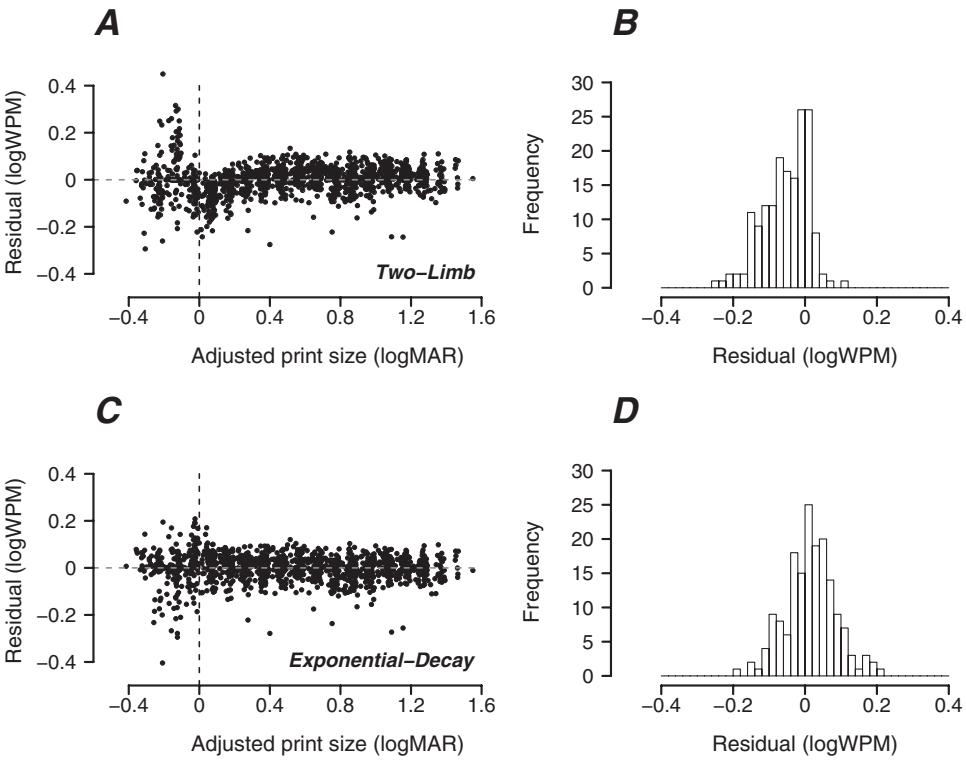

FIGURE 3. Residual plots from fitting with the two-limb function (**A**, **B**) and the exponential-decay function (**C**, **D**) for the normal-vision group. (**A**, **C**) Residual is plotted as a function of print size adjusted relative to the CPS_{TL}. (**B**) Two-limb and (**D**) exponential-decay panels are the histograms of the residuals from print sizes within 0.1 logMAR of the CPS_{TL}.

TABLE 1. Regression Coefficients and Adjusted R^2 from Regressing CPS_{TL} on CPS_{ED} for Different Criterion Levels in the Regular Contrast Polarity Data Set for the Normal-Vision Group

Threshold (% of MRS)	*y*-Intercept	Slope	Adjusted R^2
75	0.0374 (0.0233,0.0505)	0.956 (0.857,1.075)	0.853 (0.729,0.914)
80	0.0670 (0.0518,0.0816)	0.996 (0.882,1.131)	0.836 (0.704,0.903)
85	0.1041 (0.0867,0.1213)	1.047 (0.905,1.200)	0.806 (0.655,0.886)
90	0.1547 (0.1336,0.1760)	1.116 (0.930,1.299)	0.757 (0.576,0.858)
95	0.2387 (0.2108,0.2679)	1.230 (0.968,1.469)	0.673 (0.445,0.812)

panels (B and D) of Figure 3 show histograms of the residuals for print sizes within 0.1 logMAR (i.e., one line on the MNREAD chart) of the CPS_{TL} in the normal-vision data set. The means of the residuals around the CPS_{TL} were −0.054 (−0.064, −0.045) logWPM and 0.016 (0.006, 0.027) logWPM for TL fits and ED fits, respectively. In other words, the TL fits overestimated the reading speed, whereas the ED fits underestimated it, but to a lesser extent, near the critical print size.

Critical Print Size from ED Fits (CPS_{ED}) versus Critical Print Size from TL Fits (CPS_{TL})

Table 1 shows the regression coefficients and the adjusted R^2 for linear regressions of CPS_{ED} for different reading speed criteria (75%–95% of the MRS) versus CPS_{TL} for regular polarity. The linear regression results for the reverse polarity data set were similar to those for the regular polarity data set and are not shown here. Not surprisingly, the correlations between CPS_{ED} for different criteria and CPS_{TL} were high (adjusted R^2 varies from 0.673 to 0.853 for regular polarity and from 0.653 to 0.765 for reverse polarity). Although regression with a CPS_{ED} criterion of 75% gave the highest adjusted R^2 values, CPS_{ED} criterion of 85% yielded slopes that were closest to 1. A slope of ~1 makes the conversion between CPS_{ED} and CPS_{TL} straightforward as a mere offset (the *y*-intercept). For instance, given that the slope is close to 1 for CPS_{ED} criteria of 80% and 85%, the *y*-intercept is approximately the average difference between the CPS_{ED} and CPS_{TL}. A CPS_{ED} criterion of 80% is a good compromise for high adjusted R^2 and slope ~1. Figure 4 shows the data and the regression line for CPS_{ED} with a criterion level of 80% versus CPS_{TL} for the regular polarity data set.

NLME Modeling of Complete and Incomplete MNREAD Data Sets

Figure 5A shows a scatter plot of RMS errors from NLME model fitting (RMS_{NLME}) against the RMS errors from individual curve fitting (RMS_{IND}) with the exponential-decay function. RMS errors fall almost perfectly on the equality line. The mean differences of $RMS_{NLME} - RMS_{IND}$ were 0.0025 (0.0017, 0.0040) logWPM for regular polarity and 0.0020 (0.0016, 0.0029) logWPM for reverse polarity.

For both contrast polarities, data were missing in 22 of 42 data sets on the rising part of the MNREAD curve. Figure 6 shows the truncated data sets for the regular contrast polarity. For the truncated sets with missing data on the rising part, 66% of data points remained in the data sets on average (number of remaining data points varied from 8 to 13). For the truncated sets with missing data on the asymptote, 34% of data points remained in the data sets on average (number of remaining data points varied from 4 to 7).

Figure 5B shows a scatter plot of RMS errors from an NLME model fitting against the RMS errors from individual curve fitting with the exponential-decay function for the truncated data sets. The mean differences of $RMS_{NLME} - RMS_{IND}$ were 0.0053 (0.0035, 0.0091) logWPM for regular polarity and 0.0084 (0.0058, 0.0121) logWPM for reverse polarity. The fitted curves for the regular polarity data sets are shown in Figure 6. Given a relatively complete data set, individual curve fitting will often have better fits because estimation of individual parameter sets from NLME modeling is constrained by the estimated means (fixed effects) and variances (random effects) of the groups.

RMS errors were calculated when applying the parameter estimates from the truncated data sets to predict the missing data. Figure 5C shows a scatter plot of RMS prediction errors from NLME model fitting against the RMS prediction errors from individual curve fitting with the exponential-decay function. (Nine data points [11%] with extreme values, which had RMS_{IND} >6 logWPM, are not shown on the plot. These extreme values were usually a consequence of problematic predictions of the missing data on the rising part of the reading speed curve.) We used median values to summarize the RMS prediction errors to limit the biases introduced by the extreme values. Median differences of $RMS_{NLME} - RMS_{IND}$ were −0.09 (−0.16, −0.03) logWPM for regular polarity and −0.06 (−0.10, −0.04) logWPM for reverse polarity.

Figure 7 shows our AMD data set with curves fitted with NLME modeling (solid lines) and with individual curve fitting (dashed lines). NLME modeling and individual curve fitting often produced similar parameter estimates. However, in some cases, individual curve fitting produced unrealistic parameter estimates. For example, for AMD10, the estimated MRS and

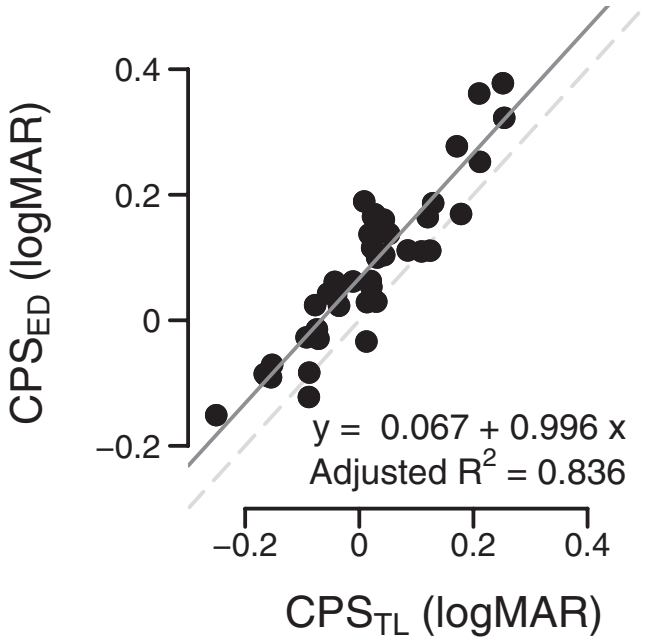

FIGURE 4. Regression of CPS from the ED fits (CPS_{ED}) against critical print size from the TL fits (CPS_{TL}) for the regular polarity data set for the normal-vision group. The criterion level for CPS_{ED} is 80% of the MRS. The regression line is drawn as the *solid line*. The equality line is drawn as a *dashed line*.

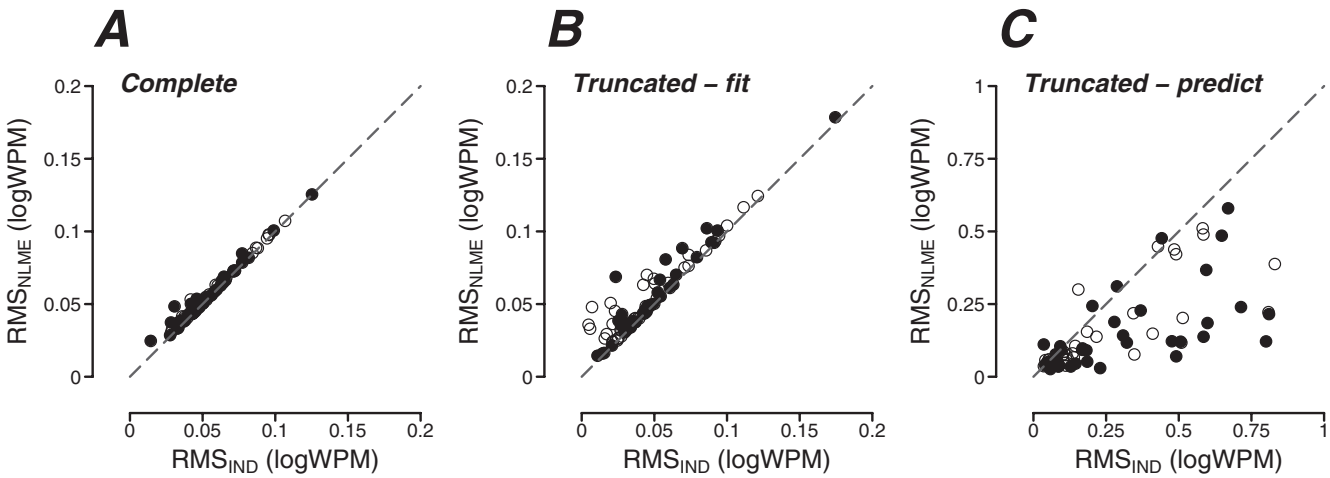

FIGURE 5. Plots of RMS errors from NLME model fits (RMS_{NLME}) against RMS errors from individual curve fits (RMS_{IND}) for the normal-vision group. Data from the regular contrast polarity (black on white) data set are plotted as *filled circles*. Data from the reverse contrast polarity (white on black) data set are plotted as *open circles*. The *dashed line* is the equality line. (**A**) RMS errors from NLME modeling of the normal-vision data set with the exponential-decay function. (**B**) RMS errors from fitting the truncated data sets. (**C**) RMS errors from predicting the missing data in the truncated data sets.

CPS_{ED} (80% of MRS) from individual curve fitting were 7.21 logWPM and 19.82 logMAR, respectively, whereas those from NLME modeling were 2.15 logWPM and 2.20 logMAR. Table 2 shows the estimated MRS and CPS_{ED} (80% of MRS) from individual curve fitting and NLME modeling for each of the 14 AMD patients.

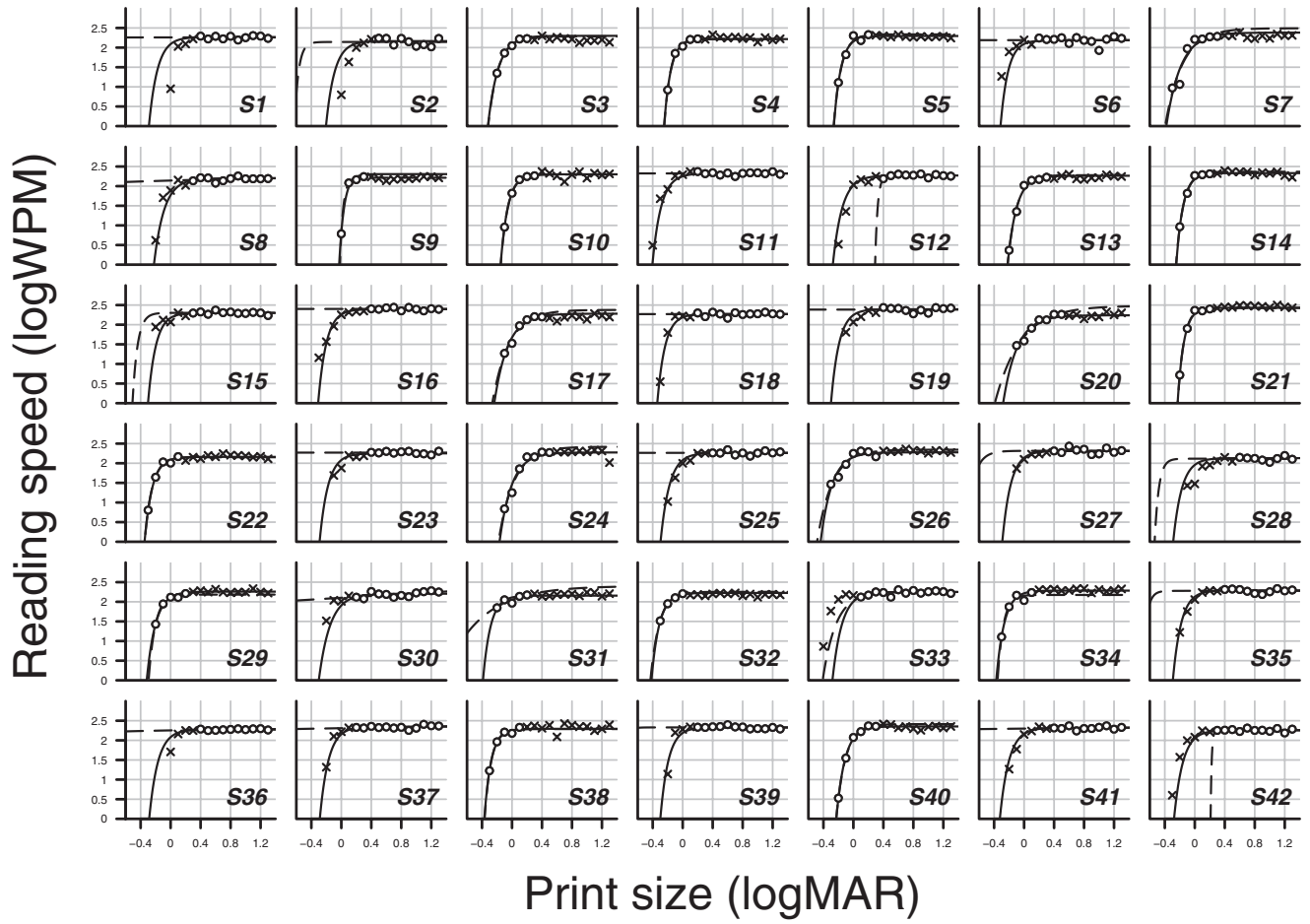

FIGURE 6. Truncated data set (regular polarity) for the normal-vision group. Each panel shows the data from one observer. Missing data were plotted as *crosses* and the remaining data as *open circles*. The *solid line* is the estimated curve from NLME modeling. The *dashed line* is the estimated curve from individual curve fitting.

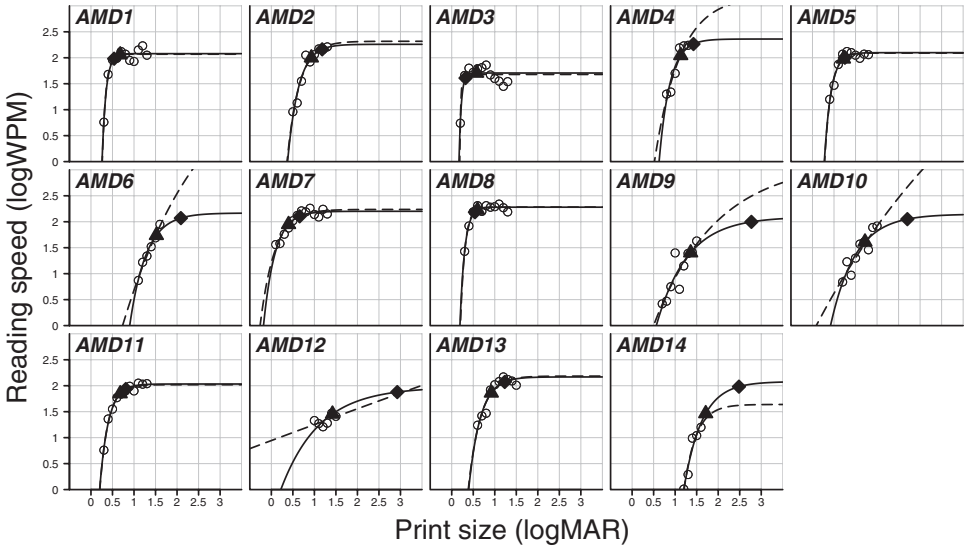

FIGURE 7. Fitted curves for the AMD data set. Each panel shows the data from one observer. The *solid line* is the estimated curve from NLME modeling. The *dashed line* is the estimated curve from individual curve fitting. CPS_{ED} values are plotted as *solid diamonds*, and the *solid triangles* are suggested print sizes from the fixed-acuity reserve (0.3 logMAR) method.

DISCUSSION

The exponential-decay function fits for reading speed versus print size data are reliably better than the two-limb function fits, but the differences in the overall goodness-of-fit are small. However, the exponential-decay function did not involve the same problem of underestimating the CPS inherent in the two-limb function. Thus, fitting with the exponential-decay function has potential advantages over the two-limb function in MNREAD parameter estimation.

On the other hand, the simplification of the curve into two straight lines in the two-limb function may be easier for researchers and clinicians to understand and interpret. In clinical settings, the straight lines can often be fitted by eye. Parameter estimation with the exponential-decay function relies on optimization techniques using computer software.

The exponential-decay function provides a slightly better fit to the MNREAD curves than the two-limb function but requires selection of a criterion for the CPS. We found that a CPS_{ED} of 80% of MRS yielded print sizes slightly larger (0.07 logMAR) than the CPS_{TL} values from the two-limb fit. Adopting a more conservative CPS_{ED} criterion of 90% MRS produced print sizes averaging 0.15 logMAR larger than the CPS_{TL}. When a clinician prescribes a reading magnifier for a patient with visual impairment, the goal is usually for the magnified print to be at least as large as the CPS for the patient to achieve MRS.[33,34] Whittaker and Lovie-Kitchin defined "acuity reserve" as the ratio of the print size intended for reading to the acuity print size.[35] If the acuity reserve is insufficient, reading speed will be compromised. The CPS_{TL}, estimated from the two-limb fit, often underestimates the print size required for reading at the MRS. As a result, magnifier prescription based on the CPS_{TL} estimate may underestimate the magnification required for best reading performance. Magnifier prescription based on the CPS_{ED}, with the criterion of either 80% or 90% of MRS, is more likely to yield adequate reading performance than magnifier prescription based on the CPS_{TL} from the two-limb fit.

Clinicians could modify the CPS_{ED} criterion, depending on circumstances. For example, a higher criterion could be used for fluent or maximum reading, whereas a lower criterion could be used for spot reading.[35] A lower criterion would correspond to a smaller print size, lower magnification, and perhaps slower reading. A higher criterion would correspond to higher magnification and closer approximation to maximum reading speed.

Cheong et al.[36] suggested a fixed-acuity-reserve (0.3 log unit) method to determine the magnification needed by low-vision patients. Table 3 shows the CPS_{ED} (80% of MRS) along with the suggested print size using the fixed-acuity-reserve method ($PS_{reserve}$) and their corresponding reading speeds. The CPS_{ED} and the $PS_{reserve}$ are also plotted in Figure 7. In general, the CPS_{ED} suggests a larger print size compared with the fixed-acuity-reserve method. It should be noted that for some patients, the CPS_{ED} is larger than 1.5 logMAR and might already have reached the declining portion of the reading-speed curve for very large print sizes. However, it is unclear whether AMD patients experience the same downturn as normally sighted people or whether it sets in at the same logMAR values. In most cases, magnifier prescription based on the CPS_{ED} may result in better reading performance than the fixed-acuity reserve method. Magnification based on the CPS_{ED} provides a good starting point in the performance trial process of magnifier prescription. Thus, it helps reduce the consulting time and frustration for trial and error in the magnifier prescription process.

TABLE 2. Estimated Maximum Reading Speed (MRS) and Critical Print Size for Reading (CPS_{ED}, 80% of MRS) from Individual Curve Fitting and NLME Modeling for Each of the 14 AMD Patients

	Individual Curve Fitting		NLME Modeling	
	MRS (logWPM)	CPS_{ED} (logMAR)	MRS (logWPM)	CPS_{ED} (logMAR)
AMD1	2.07	0.52	2.08	0.54
AMD2	2.32	1.27	2.26	1.18
AMD3	1.68	0.25	1.71	0.32
AMD4	3.19	2.59	2.36	1.43
AMD5	2.09	0.73	2.10	0.75
AMD6	5.25	8.35	2.17	2.09
AMD7	2.24	0.79	2.20	0.66
AMD8	2.28	0.52	2.28	0.54
AMD9	3.16	5.57	2.09	2.77
AMD10	7.21	19.82	2.15	2.20
AMD11	2.02	0.79	2.03	0.81
AMD12	29.82	531.70	1.97	2.93
AMD13	2.19	1.26	2.17	1.23
AMD14	1.64	2.00	2.08	2.48

TABLE 3. Estimated Critical Print Size for Reading (CPS_{ED}) and Its Corresponding Reading Speed (80% of MRS) from NLME Modeling and Suggested Print Size Using the Fixed-Acuity-Reserve Method ($PS_{reserve}$) and Its Corresponding Reading Speed (Predicted from the Fitted Curve) for Each of the 14 AMD Patients

	NLME Modeling		Fixed-Acuity-Reserve Method	
	CPS_{ED} (logMAR)	Reading Speed (logWPM)	$PS_{reserve}$ (logMAR)	Reading Speed (logWPM)
AMD1	0.54	1.98	0.68	2.06
AMD2	1.18	2.16	0.93	2.00
AMD3	0.32	1.61	0.58	1.71
AMD4	1.43	2.26	1.13	2.04
AMD5	0.75	2.00	0.72	1.98
AMD6	2.09	2.07	1.52	1.74
AMD7	0.66	2.10	0.40	1.95
AMD8	0.54	2.18	0.60	2.22
AMD9	2.77	2.00	1.36	1.40
AMD10	2.20	2.05	1.22	1.61
AMD11	0.81	1.94	0.68	1.85
AMD12	2.93	1.88	1.42	1.46
AMD13	1.23	2.07	0.92	1.86
AMD14	2.48	1.98	1.71	1.46

In a typical MNREAD data set, there are usually fewer data points on the rising slope of the curve than on the asymptote. Thus, the estimation of the slope in the two-limb function and the rate of change in the exponential-decay function can be noisy. Moreover, acuity reduction and inadequate testing time in clinical settings often result in a sparse MNREAD data set for individual patients. Our results show that NLME modeling can be used to estimate reading speed and critical print size in cases of sparse data as long as there are supporting data from a group of similar observers. Based on Figures 6 and 7, which show fitted curves to the incomplete data sets, the fits seem better when the measured data are on the rising slope than on the asymptote. For instance, in Figure 6, only four data points resulted in reasonable curve fits for the S9 and S32 data sets. Thus, from the perspective of data analysis and parameter estimation, it would be beneficial to measure reading speed starting from small print near the reading acuity limit and proceed to larger print sizes, gathering points on the rising part of the reading speed curve.

Our results indicate that NLME modeling may prove useful in clinical data sets in which individual data are noisy or incomplete. In such cases, NLME parameter estimates may have higher prediction accuracy than the parameters estimated from individual curve fitting. Further verification of the benefits of NLME modeling with larger MNREAD data sets among different kinds of patients is needed. Our preliminary analysis of MNREAD data from 341 older persons with and without cataract shows promising results (Kallie CS. *IOVS* 2005;46: ARVO E-Abstract 4589). In its current form, NLME modeling may not be easily accessible to many clinical practitioners. However, it is possible to make NLME modeling through a Web page interface. A Web-based version of the statistical software used is available (http://rweb.stat.umn.edu/Rweb/), which means model fitting can be performed on any regular computer with Web access.

CONCLUSIONS

NLME models use the information from population estimates and provide good fits to individual data sets. This approach can also be used to compare response curves, either for different experimental conditions in the same observer[37] or for different observers from different populations and different patient groups (Kallie CS. *IOVS* 2005;46:ARVO E-Abstract 4589), in psychophysical studies.

We have shown that (1) the exponential-decay function is better than the two-limb function for fitting MNREAD data, (2) NLME models can be a useful method of analyzing grouped reading speed versus print size data, and (3) the predicted set of parameters for each observer from NLME modeling predicts the data reasonably well, even for incomplete data sets. The last point is important for clinical MNREAD data, which is often incomplete because of acuity reduction or testing time limitations. Our demonstration of the merits of NLME modeling for MNREAD data indicates the potential value of NLME modeling for other types of clinical vision testing.

APPENDIX

Nonlinear Mixed-Effects Models of Reading Speed Data

The NLME models are specified as follows[5,6]:

$$y_{ij} = f(x_{ij},\mathbf{\Phi}_i) + \varepsilon_{ij}, \varepsilon_{ij} \sim N(0,\sigma^2),\ i = 1,\ldots,n, j = 1,\ldots,m_i$$

where y_{ij} is the reading speed in logWPM at the jth print size x_{ij}, $f(x_{ij}, \mathbf{\Phi}_i)$ and is either the *two-limb* function or the *exponential-decay* function with parameter vector $\mathbf{\Phi}_i$ for the ith observer. ε_{ij} is the residual error, which follows the normal distribution with mean zero and variance σ^2. The parameter vector $\mathbf{\Phi}_i$ determines the reading speed curve for each observer, and is modeled as:

$$\mathbf{\Phi}_i = \boldsymbol{\beta} + \boldsymbol{b}_i, \boldsymbol{b}_i \sim \mathrm{N}(\mathbf{0},\boldsymbol{\psi})$$

where $\boldsymbol{\beta}$ is the mean parameter vector and $\boldsymbol{b}_i$ is the vector for the random effects for the ith observer. $\boldsymbol{b}_i$ is normally distributed with a zero mean vector and variance-covariance matrix $\mathbf{\Psi}$.

More sophisticated models of the parameter vector $\mathbf{\Phi}_i$ can be formulated by replacing the mean parameter vector $\boldsymbol{\beta}$ with any fixed-effect structure of interest and the random-effect vector $\boldsymbol{b}_i$ with the corresponding more complex random-effect structure. In our first analysis, we had fixed effects of contrast polarity and random effects of both contrast polarity and individual variations. The same model was also fitted to the truncated data sets. Another NLME model with a mean parameter vector and random effects of individual variations was used to analyze the data sets from our patients with AMD. After fitting an NLME model, the parameter vector $\mathbf{\Phi}_i$ for each observer was estimated with best linear unbiased predictor, or BLUP.[38,39]

Model-Fitting Implementation

All data analyses were implemented in R (http://www.r-project.org/)[40] with the NLME library.[7] The Nelder-Mead simplex algorithm[41] was used to find the parameter combinations that minimize the residual sum of squares in individual curve fitting. R scripts for fitting NLME models to our data sets are available for download at http://vision.psych.umn.edu/~gellab/mnread/.

Acknowledgment

The authors thank Kimberly McHugh for her help with data collection.

References

1. Cudeck R. Mixed-effects models in the study of individual differences with repeated measures data. *Multivar Behav Res*. 1996;31:371–403.
2. Cudeck R, Harring JR. Analysis of nonlinear patterns of change with random coefficient models. *Annu Rev Psychol*. 2007;58:615–637.
3. Audren F, Tod, M, Massin P, et al. Pharmacokinetic-pharmacodynamic modeling of the effect of triamcinolone acetonide on central macular thickness in patients with diabetic macular edema. *Invest Ophthalmol Vis Sci*. 2004;45:3435–3441.
4. Tomita G, Araie M, Kitazawa Y, Tsukahara S. A three-year prospective, randomized and open comparison between latanoprost and timolol in Japanese normal-tension glaucoma patients. *Eye*. 2004;18:984–989.
5. Lindstrom MJ, Bates DM. Nonlinear mixed-effects models for repeated measures data. *Biometrics*. 1990;46:673–687.
6. Pinheiro JC, Bates DM. Model building for nonlinear mixed-effects models. *Technical Report 91*. Madison, WI: University of Wisconsin; 1995.
7. Pinheiro JC, Bates DM. *Mixed-Effects Models in S and S-Plus*. New York: Springer; 2000.
8. Elliott DB, Trukolo-Ilic M, Strong G, Pace R, Plotkin A, Bevers P. Demographic characteristics of the vision-disabled elderly. *Invest Ophthalmol Vis Sci*. 1997;38:2566–2575.
9. Legge GE, Ross JA, Isenberg LM, LaMay JM. Psychophysics of reading, XII: clinical predictors of low-vision reading speed. *Invest Ophthalmol Vis Sci*. 1992;33:677–687.
10. Raasch TW, Rubin GS. Reading with low vision. *J Am Optom Assoc*. 1993;64:15–18.
11. Lovie-Kitchin JE, Bevan JD, Hein B. Reading performance in children with low vision. *Clin Exp Optom*. 2001;84:148–154.
12. Virgili G, Cordaro C, Bigoni A, Crovato S, Cecchini P, Menchini U. Reading acuity in children: evaluation and reliability using MNREAD charts. *Invest Ophthalmol Vis Sci*. 2004;45:3349–3354.
13. Cheong AMY, Lovie-Kitchin JE, Bowers AR, Brown B. Short-term in-office practice improves reading performance with stand magnifiers for people with AMD. *Optom Vis Sci*. 2005;82:114–127.
14. Smith HJ, Dickinson CM, Cacho I, Reeves BC, Harper RA. A randomized controlled trial to determine the effectiveness of prism spectacles for patients with age-related macular degeneration. *Arch Ophthalmol*. 2005;123:1042–1050.
15. Watson GR, Schuchard RA, De l'Aune WR, Watkins E. Effects of preferred retinal locus placement on text navigation and development of advantages trained retinal locus. *J Rehabil Res Dev*. 2006;43:761–770.
16. Legge GE, Ross JA, Luebker A, LaMay JM. Psychophysics of reading, VIII: the Minnesota low-vision reading test. *Optom Vis Sci*. 1989;66:843–853.
17. Mansfield JS, Ahn SJ, Legge GE, Luebker A. A new reading-acuity chart for normal and low vision. In: *Ophthalmic and Visual Optics/Noninvasive Assessment of the Visual System, OSA Technical Digest Series. Vol 3*. Washington DC: Optical Society of America; 1993:232–235.
18. Ahn SJ, Legge GE, Luebker A. Printed cards for measuring low-vision reading speed. *Vision Res*. 1995;35:1939–1944.
19. Mansfield JS, Legge GE, Bane MC. Psychophysics of reading, XV: font effects in normal and low vision. *Invest Ophthalmol Vis Sci*. 1996;37:1492–1501.
20. Mansfield JS, Legge GE. The MNREAD acuity chart. In: *Psychophysics of Reading in Normal and Low Vision*. Mahwah, NJ: Lawrence Erlbaum Associates; 2007:167–191.
21. Mansfield JS, Legge GE. Print size definitions and conversions. In: *Psychophysics of Reading in Normal and Low Vision*. Mahwah, NJ: Lawrence Erlbaum Associates; 2007:193–197.
22. Legge GE, Pelli DG, Rubin GS, Schleske MM. Psychophysics of reading, I: normal vision. *Vision Res*. 1985;25:239–252.
23. Legge GE, Cheung S-H, Yu D, Chung STL, Lee H-W, Owens DP. The case for the visual span as a sensory bottleneck in reading. *J Vis*. 2007;7:1–15.
24. Legge GE. Visual mechanisms in reading. In: *Psychophysics of Reading in Normal and Low Vision*. Mahwah, NJ: Lawrence Erlbaum Associates; 2007:43–105.
25. Virgili G, Pierrottet C, Parmeggiani F, et al. Reading performance in patients with retinitis pigmentosa: a study using the MNREAD charts. *Invest Ophthalmol Vis Sci*. 2004;45:3418–3424.
26. O'Brien BA, Mansfield JS, Legge GE. The effect of print size on reading speed in dyslexia. *J Res Read*. 2005;28:332–349.
27. Latham K, Whitaker D. A comparison of word recognition and reading performance in foveal and peripheral vision. *Vision Res*. 1996;36:2665–2674.
28. Subramanian A, Pardhan S. The repeatability of MNREAD acuity charts and variability at different test distances. *Optom Vis Sci*. 2006;83:572–576.
29. Cheong AMY, Legge GE, Lawrence MG, Cheung S-H, Ruff MA. Relationship between slow visual processing and reading speed in people with macular degeneration. *Vision Res*. 2007;47:2943–2955.
30. Efron B. Bootstrap methods: another look at the jackknife. *Ann Stat*. 1979;7:1–26.
31. Efron B. Nonparametric estimates of standard error: the jackknife, the bootstrap and other methods. *Biometrika*. 1981;68:589–599.
32. Efron B. Better bootstrap confidence intervals. *J Am Stat Assoc*. 1987;82:171–185.
33. Cole RG. Visual acuity and predicted reading add. In: Rosenthal BP, Cole RG, eds. *Functional Assessment of Low Vision*. St. Louis: CV Mosby; 1996:27–39.
34. Dickinson C. *Low Vision: Principles and Practice*. Boston: Butterworth-Heinemann; 1998.
35. Whittaker SG, Lovie-Kitchin JE. Visual requirements for reading. *Optom Vis Sci*. 1993;70:54–65.
36. Cheong AMY, Lovie-Kitchin JE, Bowers AR. Determining magnification for reading with low vision. *Clin Exp Optom*. 2002;85:229–237.
37. Chung STL, Jarvis SH, Cheung S-H. The effect of dioptric blur on reading performance. *Vision Res*. 2007;47:1584–1594.
38. Henderson CR. Best linear unbiased estimation and prediction under a selection model. *Biometrics*. 1975;31:423–447.
39. Robinson GK. That BLUP is a good thing: the estimation of random effects. *Stat Sci*. 1991;6:15–32.
40. Ihaka R, Gentleman R. R: a language for data analysis and graphics. *J Comp Graph Stat*. 1996;5:299–314.
41. Nelder JA, Mead R. A simplex method for function minimization. *Computer J*. 1965;7:308–313.